



Title of proposed experiment:

A Study of the  $^{15}\text{O}(\alpha,\gamma)^{19}\text{Ne}$  Reaction at the Astrophysically Important Energy

Name of group: Hotenough

Spokesperson for group: L.Buchmann

E-Mail address: LOTHAR@TRIUMF.CA

Fax number: 604-222-1074

Members of the group (name, institution, status, per cent of time devoted to experiment)

<u>Name</u>	<u>Institution</u>	<u>Status</u>	<u>Time</u>
N.Bateman	University of Toronto	Research Associate	50%
L.Buchmann	TRIUMF	Research Scientist III	50%
J.D'Auria	Simon Fraser University	Professor	50%
R. Helmer	TRIUMF	PNS	tba
D.Hutcheon	TRIUMF	Senior Research Scientist	50%
K.P.Jackson	TRIUMF	Senior Research Scientist	tba
J.D.King	University of Toronto	Professor	tba
A. Olin	TRIUMF	Senior Research Scientist	tba
P. Parker	Yale U.	Professor	tba
J.Rogers	TRIUMF	Senior Research Scientist	tba

Graduate students and postdoctoral fellows as present at the time of the experiment

Start of preparations: 1998

Beam time requested:

Date ready: 2002

12-hr shifts	Beam line/channel	Polarized primary beam?
60	ISAC-high energy	no

Completion date: 2004

In the subsequent text we propose to measure narrow resonance strengths in the  $^{15}\text{O}(\alpha,\gamma)^{19}\text{Ne}$  reaction, in particular, the well-known narrow resonances with a centre-of-mass energy of 1.076, 0.851, and 0.504 MeV, respectively. While the two upper resonances of  $^{15}\text{O}(\alpha,\gamma)^{19}\text{Ne}$  do not play a role in most explosive nucleosynthesis scenarios, the determination of their resonance strength is important as a systematic test to achieve the goal of measuring the all important strength of the  $E_R=0.504$  MeV resonance with its expected yield of 1 event/hour for a radioactive beam of  $10^{11}\text{s}^{-1}$  (16 pA). This single resonance alone determines whether the rp process will take place in a nova like environment. The measurement of the  $E_R=0.504$  MeV resonance in  $^{15}\text{O}(\alpha,\gamma)^{19}\text{Ne}$  will require that the ISAC facility can deliver both the necessary beam intensities of  $^{15}\text{O}$  as well as that a highly efficient recoil detection system is available. Details of such a proposed recoil system (DRAGON facility) are given in this and an additional report to the EEC. Certainly, this measurement is one of the biggest challenges envisaged for ISAC.

Experimental area

ISAC-high energy, recoil separator (DRAGON)

Primary beam and target (energy, energy spread, intensity, pulse characteristics, emittance)

proton (500 MeV,  $100\mu\text{A}$ )

ISAC production target (to be developed/plasma like ion source)

Secondary channel high energy ISAC beamline

Secondary beam (particle type, momentum range, momentum bite, solid angle, spot size, emittance, intensity, beam purity, target, special characteristics)

$^{15}\text{O}$ ,  $^{19}\text{Ne}$  (on-line)

stable:  $^{15}\text{N}$ ,  $^{19}\text{F}$ ,  $^{20}\text{Ne}$  from off-line ion source (OLIS)

## TRIUMF SUPPORT:

- $^{15}\text{O}$  production, target-ionsource development
- availability of  $10^{11}\text{s}^{-1}$  bunched beam of  $^{15}\text{O}$  at target
- availability of stable ion beams as specified
- $E=0.15$  to  $0.4$  MeV/u
- TRIUMF share of recoil detection facility
- data acquisition

## NON-TRIUMF SUPPORT

- NSERC part of recoil detection facility (Major Installation Grant)
- Research Project Grant for  $^{15}\text{O}(\alpha,\gamma)^{19}\text{Ne}$  project (NSERC) including PDF and graduate student support (beginning 2000)
- experiment specific modifications to recoil detection facility
- data analysis

Safety procedures for high energy experiments at ISAC are still to be worked out. However,  $^{15}\text{O}$  with a half life of 2.04 minutes and no radioactive daughter poses no particular threat compared to other possible isotopes. However, the high beam intensities will lead to the built-up of local source strengths in the Ci range while in operation. Therefore local  $\beta\gamma$  shielding at beamdump positions within the transport lines and the recoil separator will likely have to be arranged.

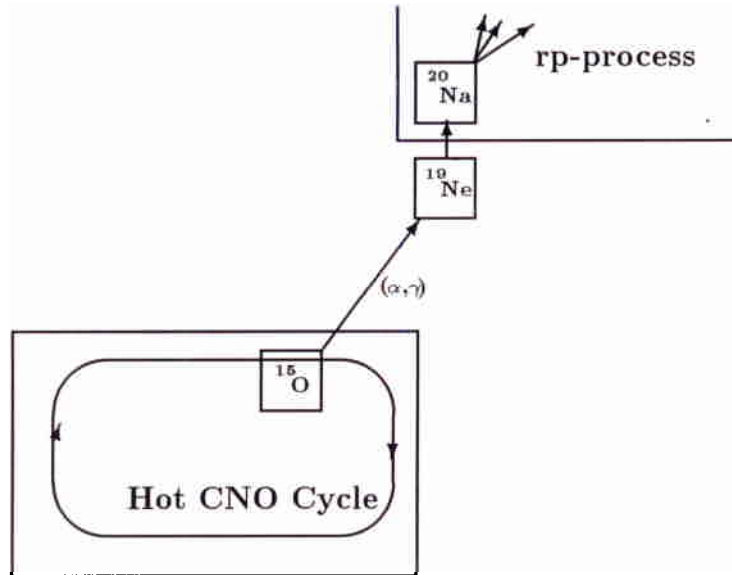


Fig. 1 The flow from the hot CNO mass region into the the rp-process mass region via the  $^{15}\text{O}(\alpha,\gamma)^{19}\text{Ne}$  reaction.

## 1 Introduction and Astrophysical Motivation

The importance of the  $^{15}\text{O}(\alpha,\gamma)^{19}\text{Ne}$  reaction for the break out from the hot CNO cycle has been first outlined by R.K.Wallace and S.E.Woosley [1] and later in several publications, most recently in ref. [2]. In short: When temperatures of about  $10^8$  K are exceeded in stellar explosions, the mass flow and energy production in the hot CNO cycle becomes restricted by the  $\beta$ -decay rates of the radioactive isotopes  $^{14,15}\text{O}$  with half lives of  $T_{1/2}=70.6$  s and 2.04 min, respectively. As a consequence most of the mass previously residing in the stable CNO isotopes (the most common ones in the universe beyond hydrogen and helium and likely enriched in a white dwarf environment) is now transformed to  $^{15}\text{O}$  and to a lesser degree to  $^{14}\text{O}$  (splitting along the half life ratio). As helium is always present in hydrogen rich matter (from the Big Bang and previous hydrogen burning in progenitor stars),  $\alpha$ -capture at  $^{15}\text{O}$  can eventually take place with a rapid  $^{19}\text{Ne}(p,\gamma)^{20}\text{Na}$  reaction to follow. This leads into the  $A \geq 20$  mass region from which there is no backflow of material into the CNO region. A schematic representation of this flow is shown in figure 1.

From these isotopes with masses  $A \geq 20$  a renewed mass flow proceeds via proton capture into the sulfur-chlorine region. Therefore both a rapid increase in energy production as well as the production of these medium heavy isotopes is encountered. Some of the isotopes produced in this scenario like  $^{26}\text{Al}$  or  $^{22}\text{Na}$  are or may be observed either directly via  $\gamma$ -rays or as isotopic anomalies in meteoric grains. This type of process, called the rp-process, takes largely place in mass accreting red giant-white dwarf binary stars, known as novae. Depending on the mass of the progenitor star of the white dwarf the white dwarf may either be composed of largely carbon or oxygen (CO-nova) or, more rarely, of oxygen, neon, and magnesium (ONeMg-Nova). The white dwarf material is assumed to be mixed with the accreting proton rich material thus giving lots of seed isotopes for

explosive burning. The discovery of ONeMg-novae has lead to speculations that the rp-process in this type of nova may start from the abundant  $^{20}\text{Ne}$  or  $^{24}\text{Mg}$ . However, about 80% of the white (ONeMg) dwarf material is  $^{16}\text{O}$  which will be transformed to  $^{15}\text{O}$  and will likely burn via  $^{15}\text{O}(\alpha,\gamma)^{19}\text{Ne}$ .

Therefore with our present nuclear knowledge it is believed that the  $^{15}\text{O}(\alpha,\gamma)^{19}\text{Ne}$  reaction rate is one of the crucial bottle necks by which the mass flow into heavier isotopes and the subsequent energy production in novae is controled. Ironically it is indeed only one state in the compound nucleus  $^{19}\text{Ne}$  which is thought to be responsible for the largest fraction of the stellar reaction rate in the temperature region around 300 million degree. Figure 2 shows the state structure of  $^{19}\text{Ne}$  as established in transfer reactions in ref. [3]. The resonance of interest is located at  $E_{cm}=504$  keV for the  $^{15}\text{O}(\alpha,\gamma)^{19}\text{Ne}$  reaction. Because of spin/channel considerations other possible resonances which contribute to the reaction rate at higher temperature are situated at  $E_{cm}=851$  and  $1076$  keV, only. Because of Coulomb penetrability reasons all these resonances are narrow, i.e. the Maxwell-Boltzmann temperature distribution in the star (and the target thickness in the experiment) integrates over them in a trivial way. In fact, the  $\gamma$ -width  $\Gamma_\gamma$  outweighs by far the  $\alpha$ -width  $\Gamma_\alpha$  for these resonances. Then the stellar reaction rate  $\langle \sigma v \rangle$ , which is the folding of the Maxwell-Boltzmann distribution with the reaction cross section, is

$$\langle \sigma v \rangle \sim \omega\gamma \exp\left(\dots \frac{E_R}{T}\right) \quad (1)$$

with the integrated resonance strength  $\omega\gamma = 2 \times \Gamma_\alpha^{-1}$  and the resonance cm energy  $E_R$ .

For any radioactive nucleus produced in stars  $\beta$ -decay and radiative capture reactions are in competition. While the  $\beta$ -decay rate is independent of the stellar temperature<sup>2</sup>, the strong dependence of  $\langle \sigma v \rangle$  of the burning temperature marks a line in the  $\rho$ -T phase diagram where both processes are of equal likelihood to occur. To obtain such a line, however, the resonance strengths  $\omega\gamma$  have to be known. For the  $E_{cm}=504$  keV resonance we take the value of  $\Gamma_\alpha=9 \mu\text{eV}$  as recently published in Ref. [4] based on a  $^{15}\text{N}(^6\text{Li,d})^{19}\text{F}$  analog transfer reaction; for the  $E_{cm}=851$  keV resonance no value is known, we take abitrarily  $\omega\gamma=1$  meV; for the  $E_{cm}=1076$  keV resonance we take  $24.5$  meV as derived in Ref. [5]. For these values  $\omega\gamma$  the  $\beta$ -capture equilibrium lines as shown in figure 3 are derived.

As novae averaged exploding temperatures and densities typically range in the  $T_8=2-3.5$ ,  $\rho=100-10000$  g/cm<sup>3</sup> hydrodynamic region, it is obvious from figure 3 that only the  $E_{cm}=0.504$  MeV resonance is of any importance in controlling the rp-process mass flow and energy production in novae. The rp break out happens actually at somewhat lower temperatures as decaying  $^{15}\text{O}$  is quickly recycled through the hot CNO cycle.

Commenting on the experimental value of  $\Gamma_\alpha$  ( $\Gamma_\alpha=9 \mu\text{eV}$ ) derived in Ref. [4]: while the state structure of  $^{19}\text{Ne}$  is well established, it is known that e.g. lithium transfer reactions to explore the  $^{12}\text{C}(\alpha,\gamma)^{16}\text{O}$  stellar reaction are unreliable when compared to results otherwise obtained [6]. In the  $^{15}\text{O}(\alpha,\gamma)^{19}\text{Ne}$  reaction, not even the transfer reaction using the same initial and final nuclei can be employed, but the analog stable  $^{15}\text{N}$  nucleus has to be used as target. In addition, the reduced  $\alpha$ -width of the  $E_x=4.033$  MeV state in  $^{19}\text{Ne}$  deduced this

---

<sup>1</sup> $\omega\gamma = \frac{2J_R+1}{(2J_T+1)(2J_P+1)} \frac{\Gamma_\alpha \Gamma_\gamma}{\Gamma_{\alpha+\gamma}}$

<sup>2</sup>Unless there is at very high temperatures thermal population of excited states.

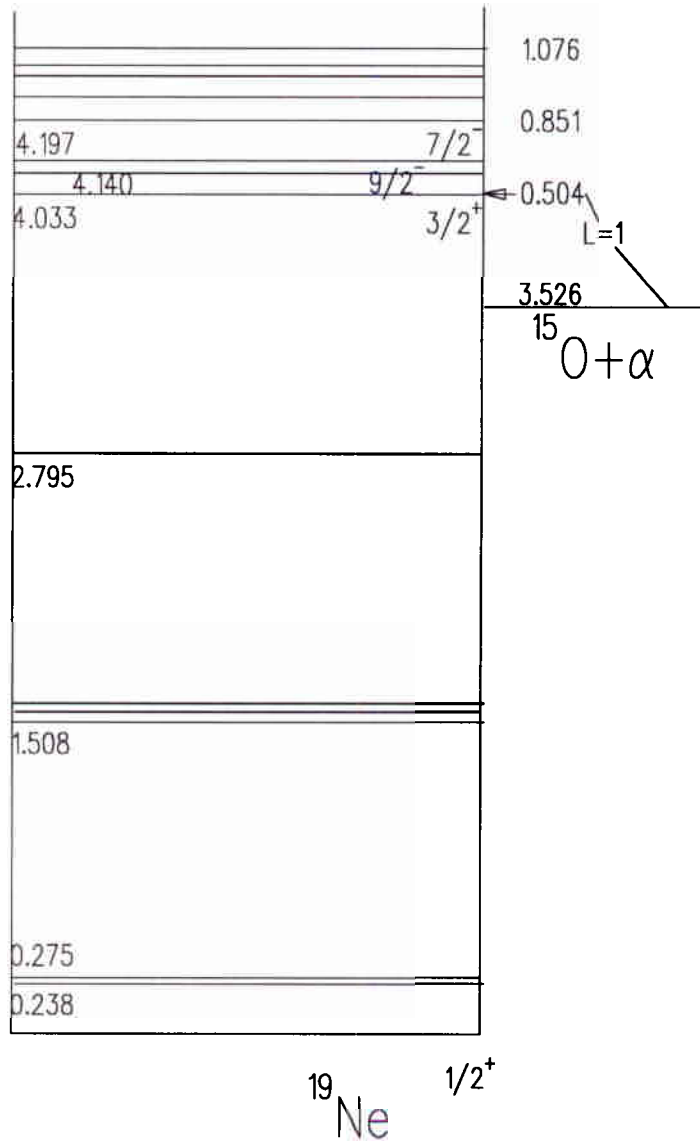


Fig. 2 The nuclear states of  $^{19}\text{Ne}$  in respect to the  $^{15}\text{O}(\alpha,\gamma)^{19}\text{Ne}$  reaction.



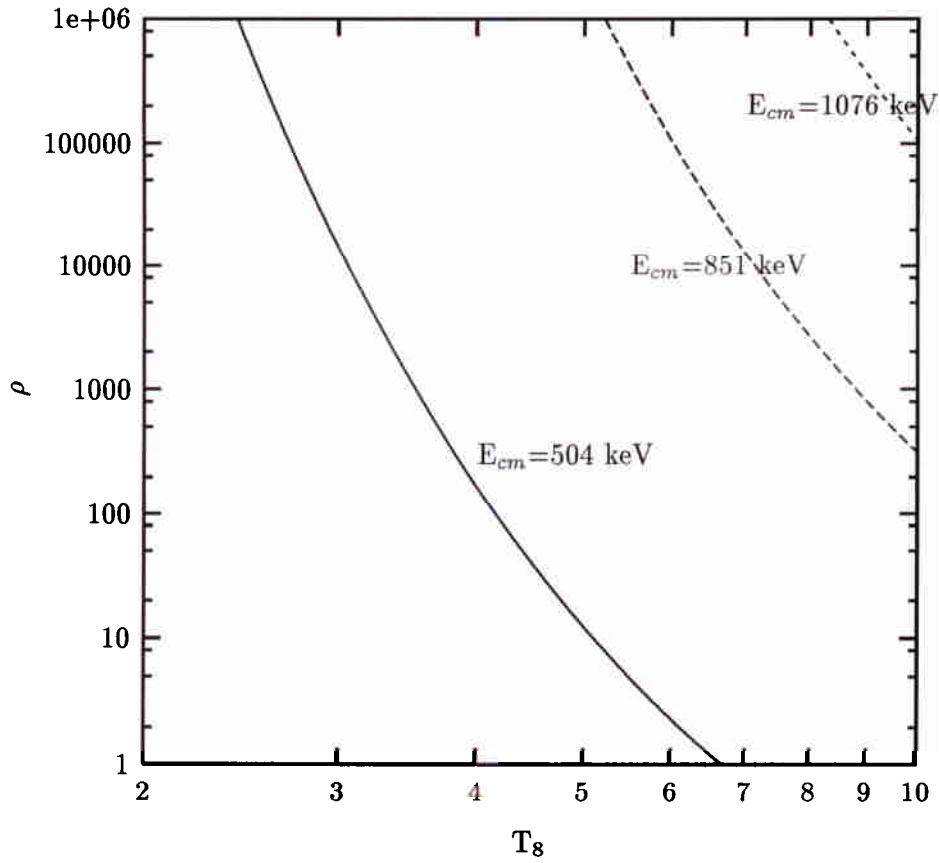


Fig. 3 Dividing line between the  $\beta$ -decay dominated  $\rho/T$  region and the  $\alpha$ -capture dominated region in  $^{15}\text{O}(\alpha,\gamma)^{19}\text{Ne}$  for the  $E_{cm}=0.504 \text{ MeV}$  resonance and  $\Gamma_\alpha=9 \mu\text{eV}$  as well as the  $E_{cm}=0.851$  and  $1.076 \text{ MeV}$  resonances, respectively. The density  $\rho$  is in units  $\text{g/cm}^3$ ,  $T_8=T/10^8 \text{ K}$ .

way is rather small, i.e. the state does not have a strong  $\alpha$ -decomposit structure. Small  $\alpha$ -widths, however, tend to make the results of transfer reactions for reduced  $\alpha$ -widths even more unreliable.

## 2 The Measurement

### 2.1 Reaction Yields

To estimate experimental yields the same resonance strengths as used in figure 3 can be employed. Resonance strength and reaction yield are connected by

$$Y = I \frac{\lambda_{cm}^2}{2} \omega \gamma \frac{1}{\epsilon_{lab}} \frac{A_T + A_P}{A_T} \quad (2)$$

with  $I$  being the incident proton current,  $\lambda_{cm}$  the de Broglie wavelength in the centre of mass system,  $\epsilon_{lab}$  the stopping power in the laboratory system and  $A$  the masses of projectile and target respectively. For a pure helium target and an  $^{15}\text{O}$  beam with an intensity of  $10^{11} \text{ s}^{-1}$  this results in a reaction yield of 1 event/hour for the  $E_{cm}=504 \text{ keV}$  resonance, with a laboratory energy of the  $^{15}\text{O}$  beam of  $0.154 \text{ MeV/u}$ . The two other resonances, situated at  $0.226 \text{ MeV/u}$  and  $0.287 \text{ MeV/u}$ , respectively, yield correspondingly: 35 events and 740 events per hour. Clearly, in a realistic experiment these two upper resonances have to be measured first. Given these yields, a detector with at least 20% background free detection efficiency is demanded. We feel that this goal can be reached with our proposed recoil detector which is subject to an EEC report and discussed in section 2.2. In fact, the design of the recoil detector is specified to fulfill the requirements of the  $^{15}\text{O}(\alpha,\gamma)^{19}\text{Ne}$  reactions. Beamtransport as well as Monte Carlo simulations for this detector are under way. From the reaction yield and the beam intensity a rejection factor above  $10^{15}$  for the detection system is required to ensure essentially background free detection. We then estimate that 10 shifts will be sufficient to map the higher lying resonances. 30 shifts are then requested for on resonance runs on the  $E_{cm}=504$  resonance to allow either for significant statistics or a meaningful upper limit on the resonance strength. 20 shifts would be used for an off-resonance control run with no  $^{19}\text{Ne}$  yield. It should, however, be noted that 20% statistical accuracy is sufficient in this experiment to derive astrophysically important conclusions.

### 2.2 A Short Description of the Recoil Particle Detection Unit

#### 2.2.1 ISAC beam properties

The ISAC accelerator picks up the beam delivered from the ISAC on-line target at  $2 \text{ keV/u}$ , i.e.  $54 \text{ keV}$  for a  $\text{C}^{15}\text{O}$  beam, and accelerates it in the first stage with an RFQ to  $150 \text{ keV/u}$ . At this energy the ionic molecule will be broken and stripped to  $^{15}\text{O}^{3+}$ . The energy of the RFQ is just below the expected resonance energy of  $E_R=154 \text{ keV/u}$ . For this low energy the subsequent DTL (linear accelerator) serves largely as a beam transport system with the magnetic quadrupoles providing transverse focussing and the bunchers conserving the time structure all through the target. A typical emittance plot for both

the longitudinal (time-energy spread) as well as the transverse emittances (position-angle,  $x,y$ ) is shown in figure 4. The longitudinal emittance is approximately  $1\text{ns}\times 0.5\%$  with tails largely in the direction of the energy spread (which can be chopped by narrow slit setting at the analysing magnet). A 0.5% energy spread corresponds to about 4 keV in the centre-of-mass of the  $A=15$  onto helium system. This spread is low enough to keep the resonances of  $E=504$  keV and  $E=536$  of  $^{15}\text{O}(\alpha,\gamma)^{19}\text{Ne}$  and  $^{15}\text{N}(\alpha,\gamma)^{19}\text{F}$ , respectively, (see section 3) safely apart.

The longitudinal emittance is about  $20\pi$  mm mrad, i.e. 4 mrad for a 5mm beamspot at target. The collimators in the gas target system (see below) will therefore allow transport with little loss to the target.

### 2.2.2 Gas target

For a helium target there is no real alternative to a windowless gas target. A windowless gas target of  $10^{18}$  atoms/cm<sup>2</sup> thickness (2 Torr, 14 cm length) will cause a slow down of 55 keV in the laboratory or 12 keV in the centre-of-mass system at the  $E_R=504$  keV resonance. One of the advantages of a windowless gas target is that it can handle any beam current. The density of a gas target is also very easy to determine by the general gas laws; the gas target is, however, an extended (linear) target which would require geometry corrections and corrections for the pressure drops through the collimators. However, for the narrow resonance case, if the beam energy is reasonably chosen, this is not the case as the resonance can be placed by the slow down of the beam into the centre of the gas target. In addition, the chemical composition of a gas target is easy to determine continuously (mass spectrometer). e.g. in elastic scattering. As the measurement of the  $^{15}\text{O}(\alpha,\gamma)^{19}\text{Ne}$  reaction is limited by the statistics achieved ( $\approx 20\%$ ) there is no major concern with the accuracy of existing stopping power tables. Figure 5 shows the windowless, extended gas target now funded by NSERC and under construction.

The gas target is designed to allow the exiting  $^{19}\text{Ne}$  recoil ions to fully escape the target and by differential pumping reach a region of high vacuum at which point the recoil separator starts. The halfcone recoil angle is given by the ratio of the  $\gamma$ - to the recoil ion momentum and is 25 mrad for the  $E_R=504$  keV resonance. A description of vacuum properties and pumping stages of the gas target can be also found in table 1.

### 2.2.3 The $\gamma$ detector array

From Ref. [7] it is clear that a coincidence between the  $\gamma$ -capture radiation and the recoiling particle will remove background in the recoil channel to a high degree. This can be achieved by several possible cuts, the first of course being the existence of such a coincidence above a low  $\gamma$ -enrhy threshold. Another cut would be on the  $\gamma$ -energy as the total  $\gamma$ -energy emitted in  $^{15}\text{O}(\alpha,\gamma)^{19}\text{Ne}$  is about 4 MeV and 80% of the decay of the  $E_R=504$  keV resonance proceed via a groundstate transition. This is considerably above several pile-up and sum signals from the  $E_\gamma=511$  keV radiation resulting from deposits of the intense  $^{15}\text{O}$  beam in the  $\gamma$ -detector region. Because of the high background radiation from these beamspills the  $\gamma$ -detector needs to be highly segmented. GEANT calculations

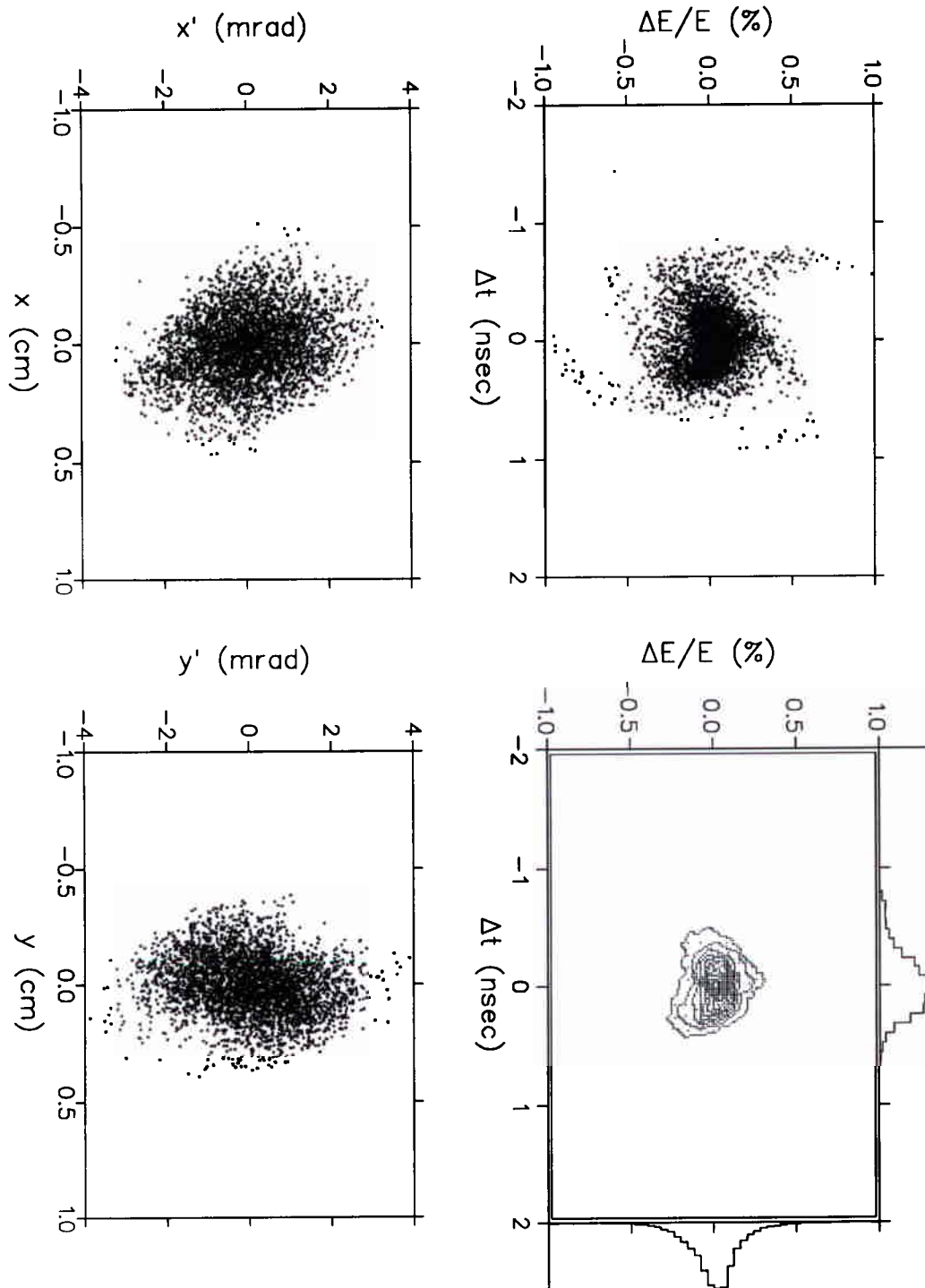


Fig. 4 Emittance plot for an  $^{15}\text{O}$  beam at target position showing both the longitudinal and transverse emittances for the x and y direction.

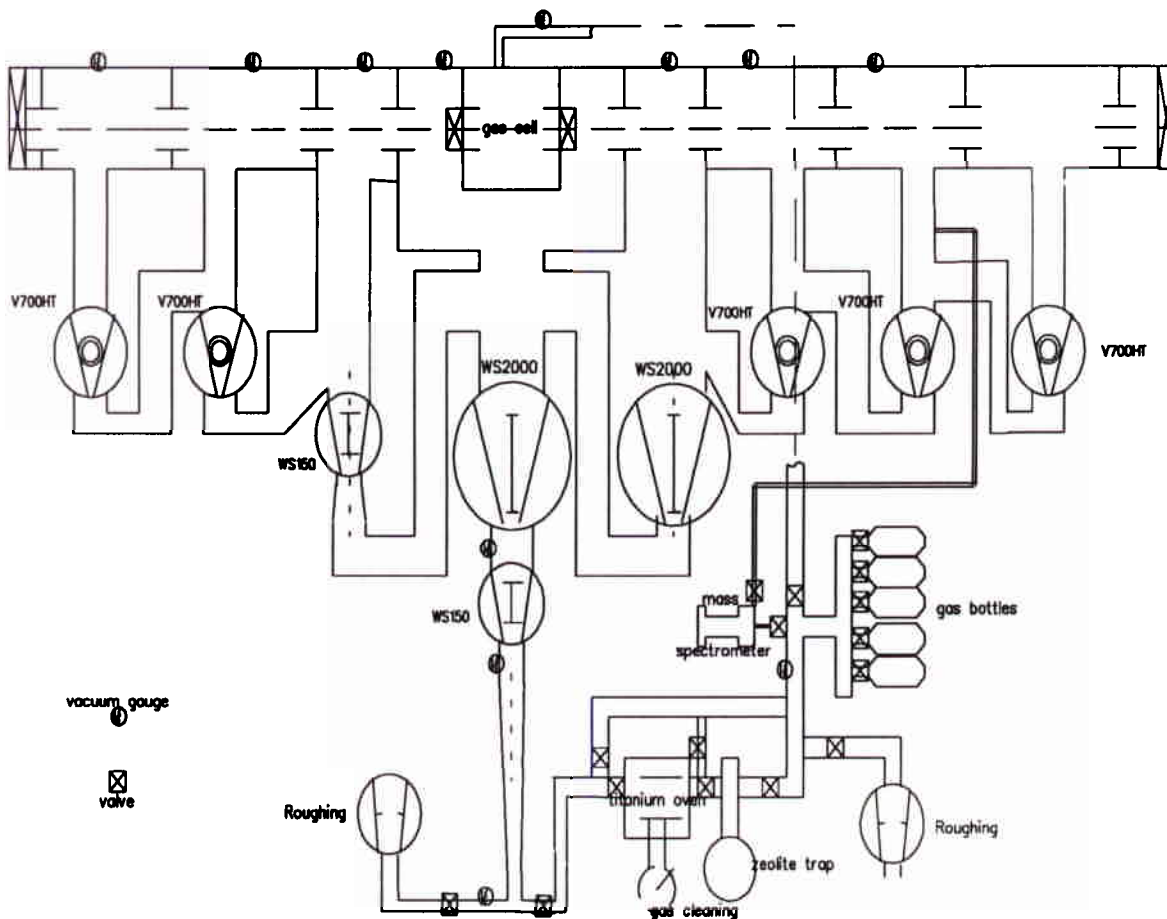


Fig. 5 The windowless, extended gas target under construction at TRIUMF.

Table 1 Description of pumping stages in the gas target for a 20 mrad exit beam opening angle. At the exit side tubes are conical. Pumping speeds are for hydrogen.

Region	Aperture tube len.	Type of flow	conductance	pump	pressure	throughput
target					1.5 T	0
central	0.8cm	viscous	31.7 l/s	WSU 2000 580 l/s	164 mT	95 Tl/s
exit 2	0.9x1.3x10cm	transit	9 l/s	WSU 2000 580 l/s	$2.1 \times 10^{-3}$ T	1.5 Tl/s
exit 3	1.44x2.0x14cm	molecu.	14 l/s	V700HT 510 l/s	$5.5 \times 10^{-5}$ T	-
exit 4	2.2x3.4x30cm	molecu.	35 l/s	V700HT 510 l/s	$3.0 \times 10^{-6}$ T	-
exit 5 <sup>1</sup>	4.1x4.9x40cm	molecu.	100 l/s	V700HT 510 l/s	$< 1 \times 10^{-6}$ T	-
entr. 2	0.8x10 cm	transit	5 l/s	Ws151 50 l/s	16.4 mT	0.8 Tl/s
entr. 3	0.8x10 cm	molecu.	2 l/s	V700HT 510 l/s	$6.4 \times 10^{-5}$ T	-
entr. 4	0.8x10 cm	molecu.	2 l/s	V700HT 510 l/s	$< 1 \times 10^{-6}$ T	-

<sup>1</sup> Fifth stage optional and integrated into the recoil separator.

indicate that about 0.3% of the beam might be dumped in the region visible to the  $\gamma$ -detector. With an acceptance geometry of 50% that would result in a rate of  $3 \times 10^8$  for the entire  $\gamma$ -detector. Given all relevant information (see J.Rogers, WEEIS proceedings), it seems to be reasonable for a quick calculation to allow a rate of  $1 \times 10^6$  per detector leading to 300 detector segments. With a spherical geometry for the  $\gamma$  detector a time resolution of 2 ns maybe achieved for a fast scintillating material, comparable to the 1 ns time structure of the beam. These beampulses come with a frequency of 11 MHz, leading to a supression factor of 45 in the pile up rate relative to a continuous beam.

With a fast-fast coincidence between the beam and the detector that would result in  $10^{-3} \text{ s}^{-1}$  in the first pile-up while about four pile ups are needed to reach the region of interest in the capture  $\gamma$ -rays. Unfortunately such very fast timing does not allow for any energy resolution of the detector. To achieve a reasonable energy resolution of the detector one has to integrate approximately the decay time of the light pulses. Therefore a fast as possible decaying scintillator (with high  $\gamma$ -efficiency) is desirable. For a BGO scintillator this decay time is about 300 ns, while for a new kind of scintillating material, called LSO, this decay constant is 47 ns. Using this new material this would lead to pile events in the first pile up of about  $5 \times 10^{-2} \text{ s}^{-1}$ . For, let's say, the third pile-up this reduces to  $1.25 \times 10^{-4} \text{ s}^{-1}$ . With a some ns timing between the  $\gamma$ -detector and the recoil ion-detector random events would be therefore highly unlikely. For the 4 MeV photopeak the highest background would then originate from cosmic rays and room background, neutron capture  $\gamma$ -radiation. Such a background, which still needs to be measured, will certainly be on a rate of several events/second or worse.

It is proposed to use techniques developed at positron emission tomography to combine the necessary high segmentation with position resolution. This would require to use rather extended LSO crystals, and cut them in a known way into fingers (optical fibres of about 7.5 cm length) and use the light output into different phototubes to encode the position of the  $\gamma$  hit. This would allow to also measure the angle of the  $\gamma$ -emission. As the recoil velocity is correlated to the angle of emittance for the  $\gamma$ -ray this technique would allow another correlation between both the time-of-flight through the recoil system and the energy of the recoil particles (dependent somewhat on the final detection system and the quality of the time focus at the end). In first approxmimation each phototube on these crystals may be considered a segment. With the discussion of pile-up rates from above one may allow then for 50 to 100 phototubes. However, as this new LSO material is under development, it is not clear at the moment, how pile-up (counting) rates, position and angular, and energy resolution do really correlate for these detectors. Therefore extensive test with one full module are necessary to decide on the possible segmentation and geometry of such a detector. More details about the  $\gamma$ -array can be found in the DRAGON report to the EEC.

#### 2.2.4 The electromagnetic separator

The electromagnetic separation system of the DRAGON facility is a two staged achromatic system employing both electric and magnetic field speration devices. Electric devices are necessary because the recoiling particle carries about the same momentum as the initial beam. The system consists of two stages, the first one leading to a separation of the initial beam and the second one removing remaining scattered particles which happen to